Published Ahead of Print on September 19, 2022 as 10.1212/WNL.0000000000201300

OPEN

Neurology®

The most widely read and highly cited peer-reviewed neurology journal
The Official Journal of the American Academy of Neurology

AMERICAN ACADEMY OF NEUROLOGY®

Neurology Publish Ahead of Print
DOI: 10.1212/WNL.0000000000201300

Association of MRI Indices of Glymphatic System With Amyloid Deposition and Cognition in Mild Cognitive Impairment and Alzheimer Disease

Author(s):
Koji Kamagata, M.D., Ph.D.[1]; Christina Andica, M.D., Ph.D.[1]; Kaito Takabayashi, B.S.[1]; Yuya Saito, M.S.[1]; Toshiaki Taoka, M.D., Ph.D.[2]; Hayato Nozaki, B.S.[1]; Junko Kikuta, M.D., Ph.D.[1]; Shohei Fujita, M.D.[1]; Akifumi Hagiwara, M.D., Ph.D.[1]; Kouhei Kamiya, M.D., Ph.D.[3]; Akihiko Wada, M.D., Ph.D.[1]; Toshiaki Akashi, M.D., Ph.D.[1]; Katsuhiro Sano, M.D., Ph.D.[1]; Mitsuo Nishizawa, M.D., Ph.D.[1]; Masaaki Hori, M.D., Ph.D.[3]; Shinji Naganawa, M.D., Ph.D.[4]; Shigeki Aoki, M.D., Ph.D.[1] on behalf of for the Alzheimer's Disease Neuroimaging Initiative

Corresponding Author:
Koji Kamagata, kkamagat@juntendo.ac.jp

Affiliation Information for All Authors: 1. Department of Radiology, Juntendo University Graduate School of Medicine, Bunkyo-ku, Tokyo 113-8421, Japan; 2. Department of Innovative Biomedical Visualization (iBMV), Nagoya University Graduate School of Medicine, Shouwa-ku, Nagoya 466-8550, Japan; 3. Department of Radiology, Toho University Omori Medical Center, Ota-ku, Tokyo 143-8541, Japan; 4. Department of Radiology, Nagoya University Graduate School of Medicine, Shouwa-ku, Nagoya 466-8550, Japan

Neurology® Published Ahead of Print articles have been peer reviewed and accepted for publication. This manuscript will be published in its final form after copyediting, page composition, and review of proofs. Errors that could affect the content may be corrected during these processes.

Equal Author Contribution:
These authors contributed equally to this work as co-first authors: Koji Kamagata, Christina Andica

Contributions:
Koji Kamagata: Drafting/revision of the manuscript for content, including medical writing for content; Major role in the acquisition of data; Study concept or design; Analysis or interpretation of data
Christina Andica: Drafting/revision of the manuscript for content, including medical writing for content; Major role in the acquisition of data; Study concept or design; Analysis or interpretation of data
Kaito Takabayashi: Drafting/revision of the manuscript for content, including medical writing for content; Analysis or interpretation of data
Yuya Saito: Drafting/revision of the manuscript for content, including medical writing for content; Analysis or interpretation of data
Toshiaki Taoka: Drafting/revision of the manuscript for content, including medical writing for content; Analysis or interpretation of data
Hayato Nozaki: Drafting/revision of the manuscript for content, including medical writing for content; Analysis or interpretation of data
Junko Kikuta: Drafting/revision of the manuscript for content, including medical writing for content; Analysis or interpretation of data
Shohei Fujita: Drafting/revision of the manuscript for content, including medical writing for content; Analysis or interpretation of data
Akifumi Hagiwara: Drafting/revision of the manuscript for content, including medical writing for content; Analysis or interpretation of data
Kouhei Kamiya: Drafting/revision of the manuscript for content, including medical writing for content; Analysis or interpretation of data
Akihiko Wada: Drafting/revision of the manuscript for content, including medical writing for content; Analysis or interpretation of data
Toshiaki Akashi: Drafting/revision of the manuscript for content, including medical writing for content; Analysis or interpretation of data
Katsuhiro Sano: Drafting/revision of the manuscript for content, including medical writing for content; Analysis or interpretation of data
Mitsuo Nishizawa: Drafting/revision of the manuscript for content, including medical writing for content; Analysis or interpretation of data
Masaaki Hori: Drafting/revision of the manuscript for content, including medical writing for content; Analysis or interpretation of data
Shinji Naganawa: Drafting/revision of the manuscript for content, including medical writing for content; Analysis or interpretation of data
Shigeki Aoki: Drafting/revision of the manuscript for content, including medical writing for content; Analysis or interpretation of data

Figure Count:
5

Table Count:
1

Search Terms:
[26] Alzheimer's disease, [39] MCI (mild cognitive impairment), [120] MRI, amyloid beta, glymphatic system

Acknowledgment:
Data collection and sharing for this project was funded by the Alzheimer's Disease Neuroimaging Initiative (ADNI) (National Institutes of Health Grant U01 AG024904) and DOD ADNI (Department of Defense award number W81XWH-12-2-0012). ADNI is funded by the National Institute on Aging, the National Institute of Biomedical Imaging and Bioengineering, and through generous contributions from the following: AbbVie, Alzheimer’s

Association; Alzheimer's Drug Discovery Foundation; Araclon Biotech; BioClinica, Inc.; Biogen; Bristol-Myers Squibb Company; CereSpir, Inc.; Cogstate; Eisai Inc.; Elan Pharmaceuticals, Inc.; Eli Lilly and Company; EuroImmun; F. Hoffmann-La Roche Ltd and its affiliated company Genentech, Inc.; Fujirebio; GE Healthcare; IXICO Ltd.; Janssen Alzheimer Immunotherapy Research & Development, LLC.; Johnson & Johnson Pharmaceutical Research & Development LLC.; Lumosity; Lundbeck; Merck & Co., Inc.; Meso Scale Diagnostics, LLC.; NeuroRx Research; Neurotrack Technologies; Novartis Pharmaceuticals Corporation; Pfizer Inc.; Piramal Imaging; Servier; Takeda Pharmaceutical Company; and Transition Therapeutics. The Canadian Institutes of Health Research is providing funds to support ADNI clinical sites in Canada. Private sector contributions are facilitated by the Foundation for the National Institutes of Health (www.fnih.org). The grantee organization is the Northern California Institute for Research and Education, and the study is coordinated by the Alzheimer's Therapeutic Research Institute at the University of Southern California. ADNI data are disseminated by the Laboratory for Neuro Imaging at the University of Southern California.

Study Funding:
Data collection and sharing for this project were funded by the ADNI (National Institutes of Health grant no. U01 AG024904) and Department of Defense ADNI (Department of Defense award number W81XWH-12-2-0012). This study was partially supported by the Juntendo Research Branding Project, JSPS KAKENHI (grant nos. JP16H06280, JP18H02772, and 19K17244), a Grant-in-Aid for Special Research in Subsidies for ordinary expenses of private schools from The Promotion and Mutual Aid Corporation for Private Schools of Japan, the Brain/MINDS Beyond program (grant no. JP19dm0307101) of the Japan Agency for Medical Research and Development (AMED), and AMED under grant number JP21wm0425006. The Department of Innovative Biomedical Visualization (iBMV), Nagoya University Graduate School of Medicine, is financially supported by Canon Medical Systems Corporation.

Disclosures:
K. Kamagata receives JSPS KAKENHI Grant Number 19K17244 and a grant from Juntendo Research Branding Project and the Brain/MINDS Beyond program (grant no. JP19dm0307101) of the Japan Agency for Medical Research and Development and is an editorial board member of BMC Neurology. C. Andica reports no disclosures relevant to the manuscripts. K. Takabayashi reports no disclosures relevant to the manuscripts. Y. Saito reports no disclosures relevant to the manuscripts. T. Taoka receives JSPS KAKENHI Grant Number 21K07563 and the Department of Innovative Biomedical Visualization (iBMV), Nagoya University Graduate School of Medicine, is financially supported by Canon Medical Systems Corporation. H. Nozaki reports no disclosures relevant to the manuscripts. J. Kikuta receives JSPS KAKENHI Grant Number 20K16737. S. Fujita reports no disclosures relevant to the manuscripts. A. Hagiwara reports no disclosures relevant to the manuscripts. K. Kamiya receives JSPS KAKENHI Grant Number 21K07629. A. Wada receives JSPS KAKENHI Grant Number 18K07730. T. Akashi reports no disclosures relevant to the manuscripts. K. Sano reports no disclosures relevant to the manuscripts. M. Nishizawa reports no disclosures relevant to the manuscripts. M. Hori receives JSPS KAKENHI Grant Number 19K08161 and is an deputy editor-in-chief of Magnetic Resonance in Medical Sciences, an editor of Neuroradiology and Japanese Journal of Radiology. S. Naganawa reports no disclosures relevant to the manuscripts. S. Aoki receives JSPS KAKENHI Grant Number 16H06280, 18H02772 and the Juntendo Research Branding Project and a Grant-in-Aid for Special Research in Subsidies for ordinary expenses of private schools from The Promotion and Mutual Aid Corporation for Private Schools of Japan, and the Brain/MINDS Beyond program (grant no. JP19dm0307101) of the Japan Agency for Medical Research and Development (AMED), and AMED under grant number JP21wm0425006.

Preprint DOI:

Received Date:
2022-02-16

Accepted Date:
2022-08-12

Handling Editor Statement:
Submitted and externally peer reviewed. The handling editor was Linda Hershey, MD, PhD, FAAN.

Abstract

Background and Objectives: The glymphatic system is a whole-brain perivascular network, which promotes CSF/interstitial fluid exchange. Alterations to this system may play a pivotal role in amyloid β (Aβ) accumulation. However, its involvement in Alzheimer's disease (AD) pathogenesis is not fully understood. Here, we investigated the changes in noninvasive MRI measurements related to the perivascular network in patients with mild cognitive impairment (MCI) and AD. Additionally, we explored the associations of MRI measures with neuropsychological score, PET standardized uptake value ratio (SUVR), and Aβ deposition.

Methods: MRI measures, including perivascular space (PVS) volume fraction (PVSVF), fractional volume of free water in white matter (FW-WM), and index of diffusivity along the perivascular space (ALPS index) of patients with MCI, those with AD, and healthy controls from the Alzheimer's Disease Neuroimaging Initiative database were compared. MRI measures were also correlated with the levels of CSF biomarkers, PET SUVR, and cognitive score in the combined subcohort of patients with MCI and AD. Statistical analyses were performed with age, sex, years of education, and *APOE* status as confounding factors.

Results: In total, 36 patients with AD, 44 patients with MCI, and 31 healthy controls were analyzed. Patients with AD had significantly higher total, WM, and basal ganglia PVSVF (Cohen's d = 1.15-1.48; $p < 0.001$), and FW-WM (Cohen's $d = 0.73$; $p < 0.05$) and a lower ALPS index (Cohen's $d = 0.63$; $p < 0.05$) than healthy controls. Meanwhile, the MCI group only showed significantly higher total (Cohen's $d = 0.99$; $p < 0.05$) and WM (Cohen's $d = 0.91$; $p < 0.05$) PVSVF. Low ALPS index was associated with lower CSF Aβ42 ($r_s = 0.41$, $p_{fdr} = 0.026$), FDG-PET uptake ($r_s = 0.54$, $p_{fdr} < 0.001$), and worse multiple cognitive domain deficits. High FW-WM was also associated with lower CSF Aβ42 ($r_s = -0.47$, $p_{fdr} = 0.021$) and worse cognitive performances.

Conclusion: Our study indicates that changes in PVS-related MRI parameters occur in MCI and AD, possibly due to impairment of the glymphatic system. We also report the associations between MRI parameters and Aβ deposition, neuronal change, and cognitive impairment in AD.

Glossary: Aβ = amyloid β; ADAS = Alzheimer's Disease Assessment Scale; ADNI = Alzheimer's Disease Neuroimaging Initiative; ALPS = diffusivity along the perivascular space; BG = basal ganglia; CDR-SB = Clinical Dementia Rating Scale Sum of Boxes; DBP = diastolic blood pressure; DTI = diffusion tensor imaging; DW = diffusion weighted; FA = fractional anisotropy; FAQ = Functional Activities Questionnaire; FDG = [^{18}F] fluorodeoxyglucose; FLAIR = fluid-attenuated inversion recovery; FSL = FMRIB Software Library 6.0.3; FW = free water; GBCA = gadolinium-based contrast agent; GMVF = gray matter volume fraction; Hipp = hippocampus; HMSCORE = Modified Hachinski Ischemic Score; ISF = interstitial fluid; MCI = mild cognitive impairment; MMSE = Mini-Mental State Examination; PVS = perivascular space; PVSVF = PVS volume fraction; RAVLT = Rey Auditory Verbal Learning Test; ROI = region of interest; SBP = systolic blood pressure; SUVR = standardized uptake value ratio; T1w = T1 weighted; WM = white matter; WML = white matter lesion; WMLVF = white-matter lesion volume fraction; WMVF = white-matter volume fraction

Footnotes: Data used in preparation of this article were obtained from the Alzheimer's Disease Neuroimaging Initiative (ADNI) database (adni.loni.usc.edu). As such, the investigators within the ADNI contributed to the design and implementation of ADNI and/or provided data but did not participate in analysis or writing of this report. A complete listing of ADNI investigators can be found at: http://adni.loni.usc.edu/wp-content/uploads/how_to_apply/ADNI_Acknowledgement_List.pdf

Introduction

The accumulation of extracellular amyloid β (Aβ), a pathological hallmark of Alzheimer's disease, is initiated >15 years before the onset of dementia.[1] This deposition results from multiple impaired brain clearance mechanisms.[2] The glymphatic system has been suggested to be an essential component of Aβ clearance in the brain of rodents.[3, 4] Glymphatic dysfunction has been found to be correlated with Aβ

accumulation; however, its involvement in the pathogenesis of Alzheimer's disease in humans is yet to be fully understood. The elucidation of its mechanism may promote new diagnostic and therapeutic methods that delay or prevent the neurodegeneration in Alzheimer's disease.

According to the glymphatic hypothesis,[5] subarachnoid CSF enters the brain interstitial space from the periarterial space via the *AQP4* channel expressed in the astrocyte end-feet and then mixes with the interstitial fluid（ISF) and waste solutes in the brain. The resulting CSF/ISF exchange and waste products, such as Aβ, are then drained out of the brain via the perivenous efflux pathway. Recent studies have demonstrated the possibility of measuring glymphatic functions using MRI, with most of them being MRI tracer–based studies using a gadolinium-based contrast agent (GBCA).[6] However, both intrathecal and intravenous GBCA administration are relatively invasive. Promising MRI-based noninvasive methods that do not require MRI tracers; namely, perivascular space (PVS) volumetry,[7] calculation of the fractional volume of free water (FW) in brain parenchyma (i.e., brain ISF) from a bitensor diffusion tensor imaging (DTI) model,[8] and calculation of the diffusivity along the PVS (ALPS) index,[9] were recently introduced for the indirect evaluation of perivascular network activity.

Although the subject remains controversial, MRI-visible PVSs are considered to reflect periarterial spaces instead of perivenous spaces. A study using 7-T MRI reported that the PVS was spatially consistent with the trajectory of small arterioles, but not venules.[10] Thus, an MRI-visible PVS corresponds to the CSF influx to the brain parenchyma of the glymphatic system. The dilatation of PVS, which is typically located in white matter (WM) at the centrum semiovale level, basal ganglia (BG), and hippocampus (Hipp), has been hypothesized to be secondary to ISF drainage blockage.[11] Neuropathological and MRI studies have reported that patients with Alzheimer's disease have a higher frequency of PVS dilatation compared with cognitively healthy participants,[12-15] a finding that was correlated with cortical Aβ deposits.[15] Most studies to date have used conventional visual scoring scales to evaluate PVSs based on the number of PVSs counted on predefined brain scan slices.[16, 17] Although a visual scoring system is relatively easy and reproducible,[18] it does not allow

for mapping the entire brain. Consequently, the methods are less sensitive and suffer from floor and ceiling effects. An automatic whole-brain PVS volume measurement methods based on isotropic three-dimensional MRI acquisition and computational imaging analyses have been proposed[19, 20] and demonstrated to correlate well with the visual rating scale using neuroradiological assessment.[19] Nevertheless, changes in the PVS volume in each anatomical predilection site in patients with Alzheimer's disease have not been fully investigated.

Estimation of the interstitial water content in the brain parenchyma, calculated as a volume fraction of FW in a voxel using a regularized bitensor model of DTI, has become possible.[8] Elevated WM FW has been reported in patients with Alzheimer's disease,[21-23] suggesting the stagnation of fluid drainage caused by glymphatic dysfunction. Using DTI, Taoka *et al.*[9] proposed the ALPS index, which is calculated from the diffusivity along the deep medullary vein at the level of the lateral ventricle body, as a measure of perivascular clearance activity in the human brain. They previously reported a significant association between the Mini-Mental State Examination (MMSE) score and ALPS index in patients with Alzheimer's disease and mild cognitive impairment (MCI). The ALPS index has also been used in the evaluation of various neurological disorders.[24-26] Furthermore, a recent study validated the ALPS index as a measure of glymphatic function.[25] Specifically, the ALPS index was found to be significantly correlated with glymphatic function measures calculated on MRI after intrathecal GBCA administration.[25]

The PVS volume is an indicator of enlargement in the periarterial space; fractional volume of FW in WM (FW-WM), a measure of brain ISF; and ALPS index, a measure of the diffusivity along the perivenular space around the deep medullary vein. Together, they enable indirect evaluation of the glymphatic system (Figure 1). We aimed to determine changes that occur in these MRI parameters in patients with MCI and Alzheimer's disease. Additionally, we examined the associations of the MRI measurements with Aβ deposition, which is thought to be caused by glymphatic dysfunction, neuropsychological scores, and PET standardized uptake value ratios (SUVRs).

Methods

Study participants

The data used in this study were obtained from the ADNI-2 database (eMethod 1 in the supplement; https://adni.loni.usc.edu). The details of the inclusion criteria, neuropsychological scores and other biomarkers assessed in the present study are available in eMethods 1–3, respectively.

MRI data acquisition

Diffusion-weighted (DW), T1-weighted (T1w), and fluid-attenuated inversion recovery (FLAIR) imaging data were acquired for each participant using a 3-T scanner. More imaging details can be found in eMethod 4 in the supplement. Furthermore, MRI data processing steps are available in eMethod 5.

PVS segmentation

PVSs were mapped from T1w images using an automated and highly reliable quantification method, following the pipeline of previous studies.[7, 27] WM lesions (WMLs), which lead to a mis-segmented PVS mask, were excluded from the PVS mask to eliminate PVS mis-segmentation caused by WM hyperintensity. The PVS volume was measured in the WM, BG, Hipp, and the sum of these structures (ALL) (Figure 2; eMethod 5 in the supplement). The PVS volume fraction (PVSVF; PVSVF = PVS volume/intracranial volume) was then obtained to eliminate interindividual variability in brain size. Details of the pipeline can be found in eMethod 6.

FW calculation

Maps of the fractional volume of FW were constructed from DW images using a regularized bitensor model with the open-source software package Diffusion Imaging in Python (also known as Dipy) algorithm (https://dipy.org/).[28] Mean cerebral FW-WM was extracted using the T1w imaging–based WM mask calculated at the MRI data processing stage (eFigure 1 in the supplement). The effects of WML and PVS were then excluded using the WML and PVS masks calculated at the MRI data processing stage.

In the process, the WML and PVS masks were registered to the DW image space by applying the FLAIR-to-T1w and T1w-to-DW image transformation matrices.

ALPS index calculation

ALPS index was calculated from DW images using a semiautomated and highly reliable pipeline developed and validated by Taoka *et al.*, [29] (Figure 3). Details can be found in eMethod 7 in the supplement. The average of the left and right ALPS indices (mean ALPS index) was then calculated. An ALPS index closes to 1.0 reflects minimal diffusivity, whereas a higher value indicates greater diffusivity.

Statistical analysis

Between-group differences in PVSVF-WM, PVSVF-BG, PVSVF-Hipp, PVSVF-ALL, FW-WM, mean ALPS index, and diffusivities in the association ($D_{xx,assoc}$, $D_{yy,assoc}$, and $D_{zz,assoc}$) and projection ($D_{xx,proj}$, $D_{yy,proj}$, and $D_{zz,proj}$) areas were evaluated using a general linear model univariate while controlling for age, sex, years of education, scanning site, and *APOE* ε4 gene carrier status (Model 1). To determine the influence of WMLs on the measurements of the glymphatic system, we also included WML volume fraction (WMLVF; WML volume/ICV) as a confounding factor in Model 2, which included the covariates of age, sex, years of education, scanning site, *APOE* ε4 gene carrier status, and WMLVF, for the evaluation of PVSVF, FW, and mean ALPS index. Furthermore, to examine the influence of changes in WM integrity on ALPS index assessment, we also included the mean FA and mean diffusivity (MD) values measured in the regions of interest (ROIs) of the association and projections fibers (eMethod 7) as a covariate for the evaluation of the ALPS index in Model 3, which included the covariates of age, sex, years of education, scanning site, *APOE* ε4 gene carrier status, WMLVF, FA, and MD. The ALPS index has been associated with gray matter (GM) atrophy in older adults with sleep disorder.[30] Considering the high incidence of GM atrophy in Alzheimer's disease, we also included GM volume fraction (GMVF; GM volume/ICV) as a confounding factor in Models 2 and 3 to create Models 4 and 5, respectively. Statistical significance was set at a *P* value of <0.05.

Finally, partial Spearman's rank correlation tests were used to evaluate the associations of MRI measurements with neuropsychological scores, CSF biomarker values, PET SUVRs, and Hipp volume adjusted for age, sex, years of education, scanning site, and *APOE* ε4 gene carrier status in the MCI and Alzheimer's disease groups combined. Notably, correlation analyses were only performed on patients with available data (Table 1). The false discovery rate was used to correct for multiple correlation tests.

Data availability

The data used in this study are publicly available in the ADNI-2 database (https://adni.loni.usc.edu). A list of the participants included in this study is available upon request to the corresponding author.

Results

Demographic and clinical characteristics of the study population

This study included 31 cognitively healthy controls (14 men and 17 women; mean age, 73.86 ± 4.91 years), 44 patients with MCI (26 men and 18 women; mean age, 73.38 ± 5.68 years), and 36 patients with Alzheimer's disease (22 men and 14 women; mean age, 74.28 ± 8.76 years) (Table 1). Age, sex, years of education, systolic and diastolic blood pressures, modified Hachinski ischemic score, and WM volume fraction (WM volume/ICV) did not vary significantly among the control, MCI, and Alzheimer's disease groups. All patients with MCI and Alzheimer's disease had a modified Hachinski ischemic score of <4, indicating primary degenerative dementia. The number of *APOE* ε4 gene carriers in the patients with MCI and Alzheimer's disease was significantly higher than controls. In contrast, no significant difference was found between the patients with MCI and those with Alzheimer's disease. Although data on neuropsychological scores, blood pressure, PET, and CSF biomarkers were not

available for all participants, at least 68% of the controls, 70% of the patients with MCI, and 83% of the patients with Alzheimer's disease had complete data.

The [^{18}F] florbetapir-PET SUVRs as well as the scores for MMSE, Montreal Cognitive Assessment, Rey Auditory Verbal Learning Test (RAVLT; immediate), and logical memory total delayed recall in the patients with MCI and Alzheimer's disease were significantly lower than controls; the same parameters in the patients with MCI were significantly lower than those in the patients with Alzheimer's disease. The [^{18}F] fluorodeoxyglucose (FDG)-PET SUVRs and RAVLT (learning and percentage of forgetting) scores in the patients with MCI and Alzheimer's disease were significantly lower than controls. The patients with Alzheimer's disease had significantly lower CSF Aβ42, CSF total tau and phosphorylated tau levels compared with controls, whereas the patients with MCI only showed a significantly lower CSF Aβ42 level compared with controls. The WMLVF and GMVF were significantly lower in patients with Alzheimer's disease than controls and patients with MCI. Functional Activities Questionnaire (FAQ), Clinical Dementia Rating Scale Sum of Boxes (CDR-SB), Alzheimer's Disease Assessment Scale (ADAS)-11, ADAS-13, and ADAS-Q4 scores in the patients with MCI and Alzheimer's disease were significantly higher than controls; the same parameters in the patients with Alzheimer's disease were significantly higher than those in the patients with MCI. The patients with Alzheimer's disease had significantly higher scores for the time to complete part B of the Trail Making Test compared with controls and patients with MCI. WMLVF, GMVF, CSF total tau and phosphorylated tau levels, RAVLT percentage of forgetting, and the score for the time to complete part B of the Trail Making Test were not significantly different between patients with MCI and controls. Moreover, FDG-PET SUVRs, RAVLT (learning and percentage of forgetting) scores, and the CSF biomarker values were not significantly different between the patients with MCI and those with Alzheimer's disease.

Between-group differences in MRI measurements

After adjusting for age, sex, years of education, scanning site, and *APOE* ε4 gene carrier status (Model 1), mean ALPS index (P = 0.026) was significantly lower and $D_{zz,assoc}$ (P = 0.006), $D_{yy,proj}$ (P = 0.003), PVSVF-WM (P < 0.001), PVSVF-BG (P < 0.001),

PVSVF-ALL ($P < 0.001$), and cerebral FW-WM ($P = 0.025$) were significantly higher in patients with Alzheimer's disease than controls (Figure 4; eFigure 2; eTable 1 in the supplement). PVSVF-ALL ($P = 0.006$) and PVSVF-WM ($P = 0.018$) were significantly higher in the patients with MCI than controls. There were no significant differences in $D_{xx,assoc}$, $D_{yy,assoc}$, $D_{xx,proj}$, $D_{zz,proj}$, and PVSVF-Hipp among the three groups; in $D_{zz,assoc}$, $D_{yy,proj}$, mean ALPS index, FW-WM, and PVSVF-BG between the patients with MCI and control participants; and in $D_{zz,assoc}$, $D_{yy,proj}$, mean ALPS index, PVSVF-ALL, PVSVF-WM, and FW-WM between the patients with MCI and those with Alzheimer's disease.

In Model 2, which included WMLVF as a covariate in addition to those of Model 1, PVSVF-WM ($P < 0.001$), PVSVF-ALL ($P < 0.001$), and PVSVF-BG ($P = 0.009$) remained significantly higher in the patients with Alzheimer's disease than controls. Significantly higher PVSVF-ALL ($P = 0.004$) and PVSVF-WM ($P = 0.007$) were also consistently observed in patients with MCI than in the healthy control participants. In addition, significantly higher PVSVF-ALL ($P < 0.001$) and PVSVF-WM ($P < 0.001$) were observed in patients with Alzheimer's disease than in those with MCI. In contrast, significant differences in PVSVF-BG observed between patients with Alzheimer's disease and those with MCI observed in Model 1 and that in FW-WM and mean ALPS index observed between patients with Alzheimer's disease and the controls were no longer present in Model 2 including the additional covariate of WMLVF.

In Model 3, which included FA, MD, and WMLVF as covariates in addition to those of Model 1, mean ALPS index ($P = 0.040$) remained significantly lower in patients with Alzheimer's disease than that among controls. Consistent with Model 1, a significant difference in mean ALPS index was not observed between patients with MCI and controls or between patients with Alzheimer's disease and those with MCI.

In Model 4, which included GMVF as a new covariate added to the covariates of Model 2, the results obtained using Model 2 were relatively preserved. PVSVF-WM ($P < 0.001$) and PVSVF-ALL ($P < 0.001$) were significantly higher in patients with Alzheimer's disease than the controls and patients with MCI, whereas PVSVF-BG ($P = 0.020$) were significantly higher in patients with Alzheimer's disease than the controls. PVSVF-ALL ($P = 0.003$) and PVSVF-WM ($P = 0.004$) remained significantly higher in

patients with MCI than the controls. No significant differences in PVSVF-BG, PVSVF-Hipp, FW-WM, and mean ALPS index were found among the three groups.

In Model 5, with GMVF included as a covariate in addition to those of Model 3, the significant difference in mean ALPS index observed among the groups in Model 1 was no longer present.

Correlation analyses

Higher PVSVF-BG was associated with worse FAQ score (r_s = 0.42, p_{fdr} = 0.026) (Figure 5; eTable 2 in the supplement). Higher FW-WM was also associated with lower CSF Aβ42 (r_s = −0.47, p_{fdr} = 0.021), worse MMSE score (r_s = −0.41, p_{fdr} = 0.021), and worse FAQ score (r_s = 0.36, p_{fdr} = 0.044). Lower mean ALPS index was associated with lower CSF Aβ42 (r_s = 0.41, p_{fdr} = 0.026), FDG-PET SUVr (r_s = 0.54, p_{fdr} < 0.001), and worse MMSE (r_s = 0.41, p_{fdr} = 0.026), FAQ (r_s = −0.38, p_{fdr} = 0.016), CDR-SB (r_s = −0.47, p_{fdr} = 0.003), ADAS-11 (r_s = −0.40, p_{fdr} = 0.013), and ADAS-13 scores (r_s = −0.33, p_{fdr} = 0.041). The correlations of PVSVF-ALL, PVSVF-WM, and PVSVF-Hipp with neuropsychological scores, CSF biomarker values, PET SUVRs, and Hipp volume were not significant.

Discussion

This study used noninvasive MRI measures to assess the whole-brain perivascular network in patients with MCI and Alzheimer's disease. The observed higher PVSVFs and FW-WM and lower mean ALPS index in patients with Alzheimer's disease as compared with control participants might reflect the dilatation of the PVS, increased extracellular free water in the WM interstitial space, and reduced water diffusivity in the perivenous spaces, possibly due to impairment of the glymphatic system. In contrast, PVSVF-ALL and PVSVF-WM changes in patients with MCI might indicate early impairment in the periarterial space. Of these measures, FW-WM and mean ALPS index were significantly associated with CSF Aβ levels, FDG-PET SUVRs, and multiple cognitive scores.

In patients with Alzheimer's disease, after adjusting for age, sex, years of education, scanning site, and *APOE* ε4 gene carrier status, PVSVF was significantly enlarged in all parts except the hippocampal region compared with the controls. This result is consistent with previous studies showing that perivascular luminal expansion in Alzheimer's disease is mainly seen in the WM (particularly in the centrum semiovale)[12-14, 20] and in some cases in the BG.[13, 14] Research has also shown that the hippocampal PVS is not associated with cognitive function or the occurrence of dementia.[31] Furthermore, in line with previous studies,[13, 32] patients with MCI only showed higher PVSVF-ALL and PVSVF-WM compared with control participants. Considering MCI as a prodromal phase of Alzheimer's disease, our results suggest that enlargement of the periarterial space occurs the earliest. Notably, the significant differences in PVSVF-ALL and PVSVF-WM between patients with Alzheimer's disease and those with MCI were only observed after the inclusion of WMLVF as a confounding factor. As expected, WMLVF was significantly higher in patients with Alzheimer's disease than in those with MCI, providing support that WMLs might contribute to an increase in the risk of Alzheimer's disease. Thus, our findings demonstrate that WMLVF should be included in the model for the evaluation of PVSVF. Although the exact cause of PVS dilation associated with Alzheimer's disease remains unknown, its pathology has been proposed to result from blockage of brain drainage pathways due to the accumulation of Aβ.[33] Indeed, Aβ deposition has also been shown to occur in the pericapillary and periarteriolar membranes, but not in the perivenular membranes.[34] The significant correlations between other MRI measures (mean ALPS index and FW-WM) and CSF Aβ observed in patients with MCI and Alzheimer's disease further suggest perivascular accumulation of Aβ as the cause of perivascular clearance impairment.

The significantly higher FW-WM in Alzheimer's disease is consistent with previously reported data.[21, 22] Here, we further showed that increases in FW-WM may reflect the stagnation of ISF drainage caused by perivascular clearance impairment. In line with a previous study,[22] our study also observed significant correlations between FW-WM and cognitive functions, such as executive function, visual construction, visuomotor coordination, and verbal performance, highlighting the effect of brain ISF accumulation on cognitive impairment. However, in contrast, the significant difference

in FW-WM between patients with MCI and control participants observed by Dumont *et al.*[21] in the same ADNI-2 cohort was not detected in this study, which might be due to the sampling size difference between our studies. In this study, we evaluated a smaller sample (31 controls, 44 patients with MCI, and 36 patients with Alzheimer's disease) relative to that examined by Dumont *et al.*[21] (81 controls, 103 patients with MCI, and 42 patients with Alzheimer's disease) because we only selected patients imaged on a GE scanner to avoid intervendor variability. Furthermore, unlike in our study, they did not consider age, sex, years of education, scanning site, and *APOE* ε4 gene carrier as confounding factors. Notably, in contrast to PVSVF, even though the normal-appearing WM without WMLs was included in the measurement of FW-WM, the significant changes in FW-WM were no longer observed after the inclusion of WMLVF as a confounding factor, indicating that the changes in FW-WM were impacted by WMLs. In the present study, WMLVF was higher in patients with Alzheimer's disease than in those with MCI and the healthy controls; therefore, small-vessel disease pathology might have also influenced the elevated FW levels detected in patients with Alzheimer's disease in the present study. Indeed, FW in normal-appearing white matter has been reported to be increased in patients with small-vessel disease.[35]

We observed a significantly reduced mean ALPS index in patients with Alzheimer's disease as compared with control participants, but we did not detect any significant difference between patients with MCI and control participants. These findings are partially consistent with those of a previous preliminary study by Steward *et al.*,[36] who comparatively evaluated the ALPS index in a small cohort of 16 patients with Alzheimer's disease, 10 patients with MCI, and 10 healthy participants using a general linear model adjusted for age, sex, and *APOE* ε4 gene status. In line with our results, they found a significant decrease in the ALPS index of patients with Alzheimer's disease; however, in contrast to our results, they found a significant decrease in the ALPS index of patients with MCI as compared with control participants. Such a discrepancy may be attributed to their small sample size (N = 36 participants) relative to ours (N = 111 participants). In addition, unlike in this study, their study did not adjust for years of education, which is an important risk factor for dementia.[37] The fact that the mean ALPS index did not significantly differ between patients with MCI

and control participants in this study suggests the relative preservation of water diffusivity in perivenous spaces in MCI. Again, a longitudinal study is essential to support our findings. Of note, the changes in the mean ALPS index were preserved even after the inclusion of FA and MD as confounding factors in multivariate analyses. Furthermore, we observed significant changes only in $D_{zz,assoc}$ and $D_{yy,proj}$ among patients with Alzheimer's disease compared with controls, reflecting increased water diffusion perpendicular to the association and projection fibers, respectively. These findings demonstrate degeneration of these fibers in Alzheimer's disease, in concurrence with the results of previous studies[38-42]. The lack of significant changes in $D_{xxassoc}$ and D_{xxproj} values suggests that the increased water diffusion perpendicular to the WM tracts is offset by reduction in water diffusion along the PVS. Therefore, the ALPS index is calculated by dividing the average of D_{xxproj} and $D_{xxassoc}$ by the average of D_{yyproj} and $D_{zzassoc}$ to eliminate the influence of diffusivity related to the WM microstructure and emphasize diffusivity along the PVS; this indicates that the ALPS index is significantly lower in the case of Alzheimer's disease. Together, we demonstrated that the change in the mean ALPS index primarily contributed by the changes in water diffusivity in the perivenous space and was not impacted by WM integrity. Nevertheless, in contrast with the other parameters included in our models, the significant changes observed in the mean ALPS index was not present after the inclusion of WMLVF and GMVF as covariates, indicating the influence of WMLs and GM atrophy on glymphatic dysfunction in MCI and Alzheimer's disease which warrants further investigation. WML pathology is considered to affect the end feet of astrocytes, leading to impairment of the glymphatic system.[43] Furthermore consistent with the findings of this study, associations between the ALPS index and regional GM atrophy were previously reported in a study of older adults,[30] which also explored the association of the ALPS index with the sleep profile and neuropsychological performance. The demonstration of an association between the ALPS index and the sleep profile and the GM volume was a strength of the study, although patients with dementia were not included. Thus, the findings of the present study, including a lower ALPS index in patients with Alzheimer's disease and the association of the ALPS index with CSF Aβ levels and multiple neuropsychological scores, complement the findings of that study.

The significant correlation between mean ALPS index and brain glucose metabolism is also worth noting. Aβ deposition was shown to cause a decrease in glucose metabolism in neurons and astrocytes that might contribute to neuronal loss.[44] Furthermore, in line with previous studies,[9, 36] we observed significant correlations between the mean ALPS index and multiple cognitive functioning scales, such as the MMSE, CDR-SB, FAQ, ADAS-11, and ADAS-13. Altogether, our findings suggest the association of glymphatic system impairment with neuronal loss, which contributes to the progression of cognitive and daily living dysfunctions in Alzheimer's disease. Furthermore, we also showed the use of the mean ALPS index as a disease progression biomarker in Alzheimer's disease.

This study has some limitations. First, the ALPS index cannot evaluate whole-brain glymphatic function. It is based on the orthogonal geometric relationship between projection and association fibers and medullary arteries and veins in the lateral ventricle body.[9] Therefore, the ALPS can only be evaluated at the level of the lateral ventricle body. Notably, the ALPS index does not exclusively measure the diffusivity of the perivenous space around the deep medullary vein—that is, it is also influenced by the surrounding white-matter microstructure included in the ROI. Thus, the ALPS index needs more careful interpretation and further investigation. Second, we did not use GBCAs in measuring glymphatic functions. Although use of CSF tracers is fairly invasive, it can be considered as the current gold standard for measuring glymphatic functions.[6] However, as mentioned above, the ALPS index has been reported to highly correlate with the glymphatic function measures calculated on MRI by intrathecal GBCA administration.[25] Third, we used only T1w images for PVS segmentation. Sepehrband *et al.*[27] reported a higher number of PVSs when only T1w or T2-weighted (T2w) images were used relative to when enhanced PVS contrast images were obtained by dividing filtered images (i.e., T1w/T2w). However, no evidence suggesting a more superior image in PVS segmentation was found. In addition, all PVS masks in this study were manually checked to identify incorrect and undetected PVSs. We also acknowledge the limitations of the PVS segmentation method. Future studies should utilize high-resolution and quasi-isotropic structural MRI. Furthermore, the accuracy of PVS segmentation depends on the quality of the image preprocessing step and tubular noise might be recognized as PVS. Fourth, this study lacked histopathological

validation. Although previous studies have suggested that a higher level of FW-WM reflects ISF stasis,[45, 46] the exact histopathological process of extracellular water changes indicated by changes in FW is not fully understood yet. The changes in FW can occur via different physiological mechanisms, such as atrophy, edema, neuroinflammation, a reduction in myelin content, or modulation in the permeability of the blood–brain barrier. Fifth, we only evaluated cross-sectional data from the ADNI-2 database. Future studies should also assess longitudinal ADNI-2 data to validate the usefulness of the noninvasive glymphatic MRI measurements. Sixth, glymphatic dysfunction has been associated with sleep disorders[30]; however, in the present study, we were unable to assess the association between sleep quality and glymphatic dysfunction in patients with MCI and Alzheimer's disease due to the lack of data. Thus, future studies should also assess the potential correlation between glymphatic dysfunction and sleep disorders. Finally, we acknowledge that the evidence supporting the utility of these MRI indicators in assessing glymphatic system function remains insufficient.

In summary, we report that PVSVF and FW-WM are higher, whereas the ALPS index is lower in individuals with Alzheimer's disease, which might reflect impairment of the glymphatic system. Furthermore, our findings provide evidence of early periarterial space changes (indexed by the PVSVF), as seen in patients with MCI. Finally, our study also suggested associations between glymphatic dysfunction in Alzheimer's disease and Aβ deposition, neuronal damage, and cognitive impairment. However, considering the methodological limitations of this study, with regard to ALPS index in particular,, results should be interpreted with caution.

WNL-2022-201199_sup --http://links.lww.com/WNL/C352

WNL-2022-201199_coinvestigator_appendix -- http://links.lww.com/WNL/C353

References

1. Sperling RA, Karlawish J, Johnson KA. Preclinical Alzheimer disease-the challenges ahead. Nature reviews Neurology 2013;9:54-58.
2. Hampel H, Hardy J, Blennow K, et al. The Amyloid-beta Pathway in Alzheimer's Disease. Mol Psychiatry 2021.
3. Iliff JJ, Wang M, Liao Y, et al. A paravascular pathway facilitates CSF flow through the brain parenchyma and the clearance of interstitial solutes, including amyloid beta. Sci Transl Med 2012;4:147ra111.
4. Kress BT, Iliff JJ, Xia M, et al. Impairment of paravascular clearance pathways in the aging brain. Ann Neurol 2014;76:845-861.
5. Xie L, Kang H, Xu Q, et al. Sleep drives metabolite clearance from the adult brain. Science 2013;342:373-377.
6. Taoka T, Naganawa S. Glymphatic imaging using MRI. J Magn Reson Imaging 2020;51:11-24.
7. Donahue EK, Murdos A, Jakowec MW, et al. Global and Regional Changes in Perivascular Space in Idiopathic and Familial Parkinson's Disease. Movement disorders : official journal of the Movement Disorder Society 2021;36:1126-1136.
8. Pasternak O, Sochen N, Gur Y, Intrator N, Assaf Y. Free water elimination and mapping from diffusion MRI. Magnetic resonance in medicine 2009;62:717-730.
9. Taoka T, Masutani Y, Kawai H, et al. Evaluation of glymphatic system activity with the diffusion MR technique: diffusion tensor image analysis along the perivascular space (DTI-ALPS) in Alzheimer's disease cases. Jpn J Radiol 2017;35:172-178.
10. Bouvy WH, Biessels GJ, Kuijf HJ, Kappelle LJ, Luijten PR, Zwanenburg JJ. Visualization of perivascular spaces and perforating arteries with 7 T magnetic resonance imaging. Investigative radiology 2014;49:307-313.
11. Wardlaw JM, Smith EE, Biessels GJ, et al. Neuroimaging standards for research into small vessel disease and its contribution to ageing and neurodegeneration. The Lancet Neurology 2013;12:822-838.
12. Banerjee G, Kim HJ, Fox Z, et al. MRI-visible perivascular space location is associated with Alzheimer's disease independently of amyloid burden. Brain : a journal of neurology 2017;140:1107-1116.
13. Chen W, Song X, Zhang Y, Alzheimer's Disease Neuroimaging I. Assessment of the Virchow-Robin Spaces in Alzheimer disease, mild cognitive impairment, and normal aging, using high-field MR imaging. AJNR American journal of neuroradiology 2011;32:1490-1495.
14. Hansen TP, Cain J, Thomas O, Jackson A. Dilated perivascular spaces in the Basal Ganglia are a biomarker of small-vessel disease in a very elderly population with dementia. AJNR American journal of neuroradiology 2015;36:893-898.
15. Roher AE, Kuo YM, Esh C, et al. Cortical and leptomeningeal cerebrovascular amyloid and white matter pathology in Alzheimer's disease. Mol Med 2003;9:112-122.
16. Wuerfel J, Haertle M, Waiczies H, et al. Perivascular spaces--MRI marker of inflammatory activity in the brain? Brain : a journal of neurology 2008;131:2332-2340.
17. Zhu YC, Tzourio C, Soumare A, Mazoyer B, Dufouil C, Chabriat H. Severity of dilated Virchow-Robin spaces is associated with age, blood pressure, and MRI markers of small vessel disease: a population-based study. Stroke 2010;41:2483-2490.

18. Potter GM, Chappell FM, Morris Z, Wardlaw JM. Cerebral perivascular spaces visible on magnetic resonance imaging: development of a qualitative rating scale and its observer reliability. Cerebrovasc Dis 2015;39:224-231.
19. Ballerini L, Lovreglio R, Valdes Hernandez MDC, et al. Perivascular Spaces Segmentation in Brain MRI Using Optimal 3D Filtering. Scientific reports 2018;8:2132.
20. Ramirez J, Berezuk C, McNeely AA, Scott CJ, Gao F, Black SE. Visible Virchow-Robin spaces on magnetic resonance imaging of Alzheimer's disease patients and normal elderly from the Sunnybrook Dementia Study. Journal of Alzheimer's disease : JAD 2015;43:415-424.
21. Dumont M, Roy M, Jodoin PM, et al. Free Water in White Matter Differentiates MCI and AD From Control Subjects. Front Aging Neurosci 2019;11:270.
22. Ji F, Pasternak O, Liu S, et al. Distinct white matter microstructural abnormalities and extracellular water increases relate to cognitive impairment in Alzheimer's disease with and without cerebrovascular disease. Alzheimers Res Ther 2017;9:63.
23. Maier-Hein KH, Westin CF, Shenton ME, et al. Widespread white matter degeneration preceding the onset of dementia. Alzheimers Dement 2015;11:485-493 e482.
24. McKnight CD, Trujillo P, Lopez AM, et al. Diffusion along perivascular spaces reveals evidence supportive of glymphatic function impairment in Parkinson disease. Parkinsonism Relat Disord 2021;89:98-104.
25. Zhang W, Zhou Y, Wang J, et al. Glymphatic clearance function in patients with cerebral small vessel disease. Neuroimage 2021;238:118257.
26. Kikuta J, Kamagata K, Takabayashi K, et al. An Investigation of Water Diffusivity Changes along the Perivascular Space in Elderly Subjects with Hypertension. AJNR Am J Neuroradiol 2022;43:48-55.
27. Sepehrband F, Barisano G, Sheikh-Bahaei N, et al. Image processing approaches to enhance perivascular space visibility and quantification using MRI. Sci Rep 2019;9:12351.
28. Garyfallidis E, Brett M, Amirbekian B, et al. Dipy, a library for the analysis of diffusion MRI data. Front Neuroinform 2014;8:8.
29. Taoka T, Ito R, Nakamichi R, et al. Reproducibility of diffusion tensor image analysis along the perivascular space (DTI-ALPS) for evaluating interstitial fluid diffusivity and glymphatic function: CHanges in Alps index on Multiple conditiON acquIsition eXperiment (CHAMONIX) study. Jpn J Radiol 2022;40:147-158.
30. Siow TY, Toh CH, Hsu JL, et al. Association of Sleep, Neuropsychological Performance, and Gray Matter Volume With Glymphatic Function in Community-Dwelling Older Adults. Neurology 2022;98:e829-e838.
31. Yao M, Zhu YC, Soumare A, et al. Hippocampal perivascular spaces are related to aging and blood pressure but not to cognition. Neurobiology of aging 2014;35:2118-2125.
32. Sepehrband F, Barisano G, Sheikh-Bahaei N, et al. Volumetric distribution of perivascular space in relation to mild cognitive impairment. Neurobiology of aging 2021;99:28-43.
33. Keable A, Fenna K, Yuen HM, et al. Deposition of amyloid beta in the walls of human leptomeningeal arteries in relation to perivascular drainage pathways in cerebral amyloid angiopathy. Biochim Biophys Acta 2016;1862:1037-1046.

34. Tarasoff-Conway JM, Carare RO, Osorio RS, et al. Clearance systems in the brain-implications for Alzheimer disease. Nature reviews Neurology 2015;11:457-470.
35. Duering M, Finsterwalder S, Baykara E, et al. Free water determines diffusion alterations and clinical status in cerebral small vessel disease. Alzheimers Dement 2018;14:764-774.
36. Steward CE, Venkatraman VK, Lui E, et al. Assessment of the DTI-ALPS Parameter Along the Perivascular Space in Older Adults at Risk of Dementia. Journal of neuroimaging : official journal of the American Society of Neuroimaging 2021;31:569-578.
37. Livingston G, Huntley J, Sommerlad A, et al. Dementia prevention, intervention, and care: 2020 report of the Lancet Commission. Lancet 2020;396:413-446.
38. Acosta-Cabronero J, Williams GB, Pengas G, Nestor PJ. Absolute diffusivities define the landscape of white matter degeneration in Alzheimer's disease. Brain 2010;133:529-539.
39. Pievani M, Agosta F, Pagani E, et al. Assessment of white matter tract damage in mild cognitive impairment and Alzheimer's disease. Hum Brain Mapp 2010;31:1862-1875.
40. Alves GS, O'Dwyer L, Jurcoane A, et al. Different patterns of white matter degeneration using multiple diffusion indices and volumetric data in mild cognitive impairment and Alzheimer patients. PLoS One 2012;7:e52859.
41. Li Y, Feng F, Lin P, et al. Cognition-related white matter integrity dysfunction in Alzheimer's disease with diffusion tensor image. Brain Res Bull 2018;143:207-216.
42. Mayo CD, Garcia-Barrera MA, Mazerolle EL, et al. Relationship Between DTI Metrics and Cognitive Function in Alzheimer's Disease. Front Aging Neurosci 2018;10:436.
43. Carotenuto A, Cacciaguerra L, Pagani E, Preziosa P, Filippi M, Rocca MA. Glymphatic system impairment in multiple sclerosis: relation with brain damage and disability. Brain 2021.
44. Tarczyluk MA, Nagel DA, Rhein Parri H, et al. Amyloid beta 1-42 induces hypometabolism in human stem cell-derived neuron and astrocyte networks. J Cereb Blood Flow Metab 2015;35:1348-1357.
45. Chad JA, Pasternak O, Salat DH, Chen JJ. Re-examining age-related differences in white matter microstructure with free-water corrected diffusion tensor imaging. Neurobiol Aging 2018;71:161-170.
46. Maillard P, Fletcher E, Singh B, et al. Cerebral white matter free water: A sensitive biomarker of cognition and function. Neurology 2019;92:e2221-e2231.

Table 1. Demographics of the study population

	HC N = 31	MCI N = 44	AD N = 36	*P*-value HC vs. MCI vs. AD	HC vs. MCI	HC vs. AD	MCI vs. AD
Sex (Male/Female)	14/17	26/18	22/14	0.363			
Age (years)	73.86 ± 4.91	73.38 ± 5.68	74.28 ± 8.76	0.867			
Years of education	16.29 ± 2.72	15.50 ± 2.81	15.22 ± 3.02	0.303			
APOE ε4 carriers (%; *N*, +/−)	29 (9/22)	65 (26/14)	71 (24/10)	**0.006**	**0.006**	**0.004**	1.000
MMSE (*N*)	28.97 ± 1.32 (29)	27.47 ± 1.94 (38)	23.39 ± 1.96 (36)	**<0.001**	**<0.001**	**<0.001**	**0.044**
MOCA (*N*)	26.10 ± 2.23 (29)	21.66 ± 2.91 (38)	17.28 ± 4.62 (36)	**<0.001**	**0.002**	**<0.001**	**<0.001**
FAQ (*N*)	0.10 ± 0.56 (29)	2.92 ± 3.26 (38)	15.31 ± 6.84 (36)	**<0.001**	**0.001**	**<0.001**	**<0.001**
CDR-SB (*N*)	0.03 ± 0.13 (29)	1.51 ± 0.8 (38)	4.78 ± 1.40 (36)	**<0.001**	**<0.001**	**<0.001**	**<0.001**
RAVLT-immediate (*N*)	45.93 ± 8.18 (29)	31.32 ± 8.69 (38)	21.64 ± 7.22 (36)	**<0.001**	**0.001**	**<0.001**	**<0.001**
RAVLT-learning (*N*)	5.38 ± 2.31 (29)	4.42 ± 2.23 (38)	2.08 ± 2.13 (36)	**<0.001**	**<0.001**	**<0.001**	0.438
RAVLT-forgetting (*N*)	3.59 ± 2.29 (29)	5.32 ± 2.94 (38)	4.56 ± 1.96 (36)	**<0.001**	0.373	**0.006**	0.299
RAVLT-% forgetting (*N*)	33.19 ± 23.74 (29)	69.04 ± 34.83 (38)	90.77 ± 13.37 (35)	**<0.001**	**<0.001**	**<0.001**	**0.017**
ADAS-11 (*N*)	4.72 ± 2.12 (29)	10.76 ± 4.56 (37)	20.06 ± 7.44 (36)	**<0.001**	**<0.001**	**<0.001**	**<0.001**
ADAS-13 (*N*)	7.79 ± 3.52 (29)	18.19 ± 6.63 (37)	30.03 ± 8.79 (35)	**<0.001**	**<0.001**	**<0.001**	**<0.001**
ADAS-Q4 (*N*)	2.66 ± 2.04 (29)	6.73 ± 2.43 (37)	8.47 ± 1.54(36)	**<0.001**	**<0.001**	**<0.001**	**0.027**
LDELTOTAL (*N*)	12.19 ± 3.36 (27)	5.53 ± 3.84 (36)	1.44 ± 1.84 (36)	**<0.001**	**<0.001**	**<0.001**	**<0.001**
TRABSCOR (*N*)	84.76 ± 40.78 (29)	125.61 ± 68.96 (38)	225.03 ± 91.62 (34)	**<0.001**	0.076	**<0.001**	**<0.001**
Aβ42 (pg/mL, *N*)	951.93 ± 309.55 (21)	844.82 ± 305.91 (31)	633.98 ± 246.78 (30)	**<0.001**	**0.007**	**<0.001**	0.251
T-tau (pg/mL, *N*)	212.82 ± 62.42 (21)	295.96 ± 154.03 (31)	350.56 ± 152.31 (30)	**0.003**	0.127	**0.002**	0.356
P-tau (pg/mL, *N)*	19.74 ± 6.12 (21)	28.88 ± 16.44 (31)	34.76 ± 16.17 (30)	**0.002**	0.121	**0.001**	0.276
FDG-PET SUVRs (*N*)	1.31 ± 0.12 (25)	1.25 ± 0.11 (33)	1.06 ± 0.18 (35)	**<0.001**	**<0.001**	**<0.001**	0.322
AV45-PET SUVRs (*N*)	1.08 ± 0.15 (25)	1.25 ± 0.25 (32)	1.41 ± 0.21 (36)	**<0.001**	**0.043**	**<0.001**	**0.032**

WMLVF (*N*)	0.03 ± 0.02 (31)	0.04 ± 0.02 (44)	0.05 ± 0.03 (36)	**<0.001**	0.513	**0.001**	**0.024**
WMVF (*N*)	0.30 ± 0.02 (31)	0.29 ± 0.02 (44)	0.28 ± 0.02 (36)	0.080			
GMVF (*N*)	0.40 ± 0.02 (31)	0.39 ± 0.03 (44)	0.37 ± 0.02 (36)	**<0.001**	0.168	**<0.001**	**0.001**
SBP (mmHg, *N*)	133.84 ± 11.38 (31)	132.77 ± 13.96 (44)	133.11 ± 19.18 (36)	0.898			
DBP (mmHg, *N*)	71.32 ± 7.60 (31)	73.27 ± 10.42 (44)	75.39 ± 9.62 (36)	0.308			
HMSCORE (*N*)	0.74 ± 0.68 (31)	0.75 ± 0.72 (44)	0.61 ± 0.77 (36)	0.472			

Data are presented as mean ± standard deviation unless otherwise stated. *N* represents the number of subjects for whom data was available. Bold values denote statistical significance at $P < 0.05$.

Abbreviations: Aβ, amyloid β; AD, Alzheimer's disease; ADAS, Alzheimer's Disease Assessment Scale; AV45, [^{18}F]florbetapir; CDR-SB, Clinical Dementia Rating Scale Sum of Boxes; DBP, diastolic blood pressure; FAQ, Functional Activities Questionnaire; FDG, [^{18}F]fluorodeoxyglucose; GMVF, gray-matter volume fraction; HC, healthy controls; HMSCORE, Modified Hachinski Ischemic Score; LDELTOTAL, Logical Memory Delayed Recall Total Score; MCI, mild cognitive impairment; MMSE, Mini-Mental State Examination; MOCA, Montreal Cognitive Assessment; P-tau, phosphorylated tau; RAVLT, Rey Auditory Verbal Learning Test; SBP, systolic blood pressure; SUVR, standardized uptake value ratio; TRABSCOR, time to complete part B of the Trail Making Test; T-tau, total tau; WMLVF, white-matter lesion volume fraction; WMVF, white-matter volume fraction.

Figure legends

Figure 1. Basic concepts of the proposed MRI measures for indirect noninvasive evaluation of glymphatic system compartments in healthy and pathological states. (**A**) Based on the glymphatic hypothesis, subarachnoid CSF normally enters the brain interstitial space from the periarterial space [as indexed by the PVSVF (i)] via the *AQP4* channel expressed in the astrocyte end-feet and then mixes with the ISF and waste solutes in the brain. The resulting CSF/ISF exchange [as indexed by the FW-WM (ii)] and waste products, such as Aβ, are then drained out of the brain via the perivenous efflux pathway [as indexed by the ALPS index (iii)]. (**B**) In a pathological state, such as in Alzheimer's disease, glymphatic dysfunction due to brain waste (i.e., Aβ) accumulation might cause enlargement of the PVS, increased brain extracellular FW, and decreased perivenous efflux, as reflected by the higher PVSVF (iii), higher FW-WM (ii), and lower ALPS index (iii), respectively.

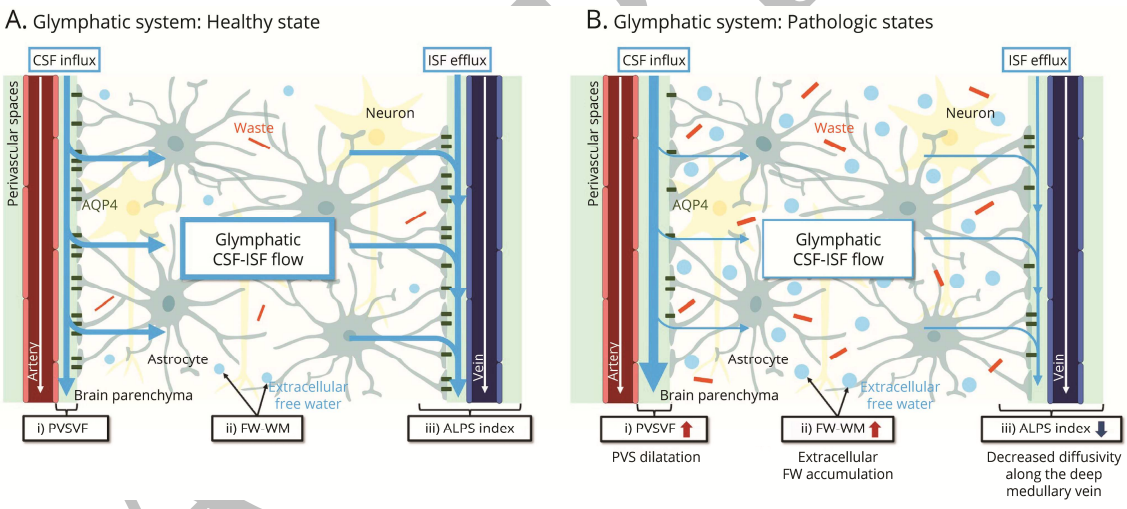

Figure 2. PVS mapping. (**A**) PVS segmentation was performed with preprocessed T1w images and by applying the Frangi filter. (**B**) PVSs were then extracted from the WM (light blue), BG (red), and Hipp (yellow).

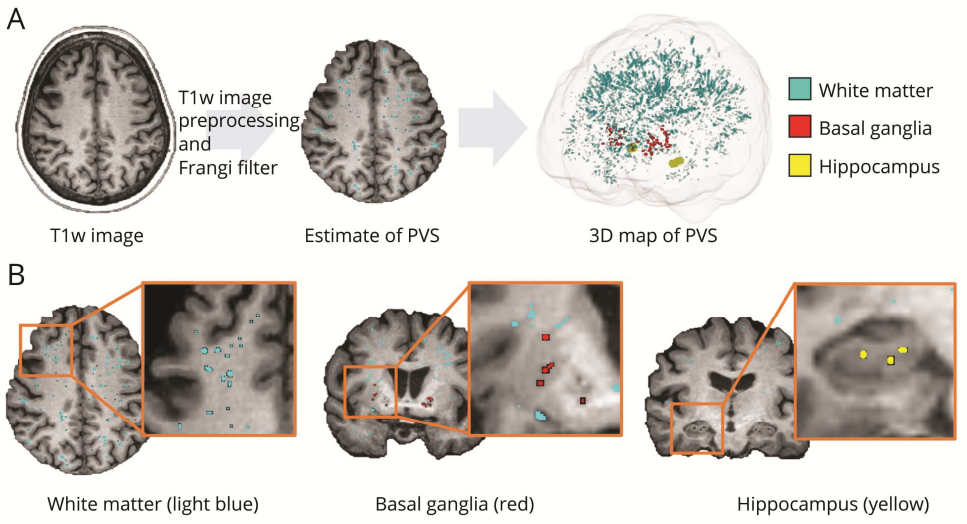

Figure 3. ALPS index calculation. (**A**) Color-coded FA map showing the distribution of the projection fibers (*z*-axis, blue) and association fibers (*y*-axis, green) at the level of the lateral ventricle of the body. Spherical ROIs measuring 5 mm in diameter were placed in the projection and association areas. Diffusion tensor is shown as an ellipsoid in the lower row. (**B**) The schematic of the geometric positional relationship of the principal fiber and PVS runs parallel to the medullary vein. The PVS runs orthogonal to the projection and association fibers. (**C**) The ALPS index was calculated as the ratio of the mean of the *x*-axis diffusivity in the projection area ($D_{xx,\mathrm{proj}}$) and *x*-axis diffusivity in the association area ($D_{xx,\mathrm{assoc}}$) to the mean of the *y*-axis diffusivity in the projection area ($D_{yy,\mathrm{proj}}$) and the *z*-axis diffusivity in the association area ($D_{zz,\mathrm{assoc}}$).

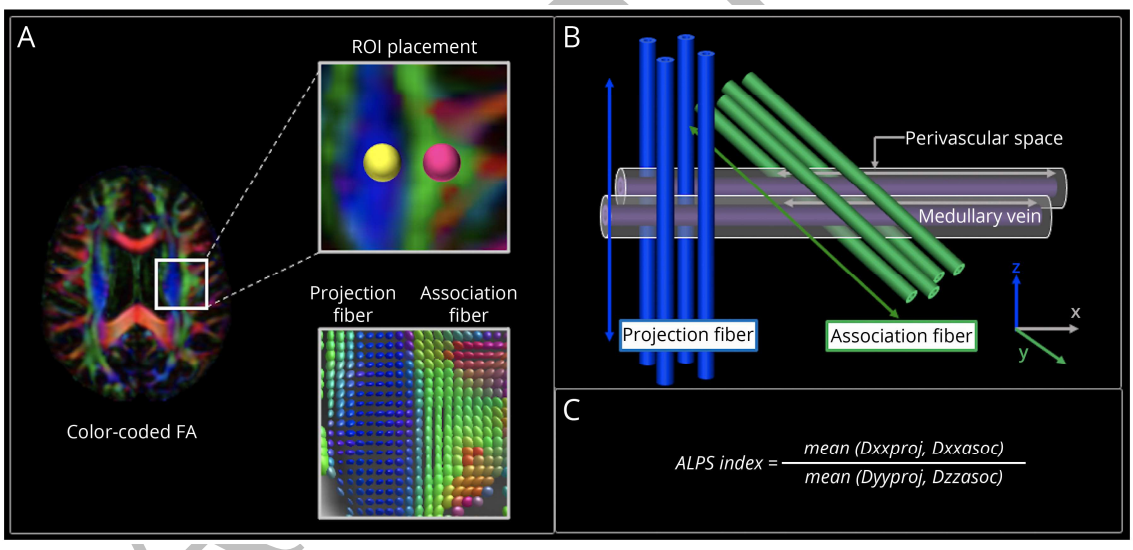

Figure 4. Between-group differences in MRI measurements. Shown are violin and box plots of the mean ALPS index, PVSVF-ALL, PVSVF-WM, PVSVF-BG, PVSVF-Hipp, and FW-WM among the healthy control (HC) participants, patients with MCI, and patients with Alzheimer's disease. The *P* values correspond to the general linear model analysis. Statistical significance was set at $P < 0.05$.

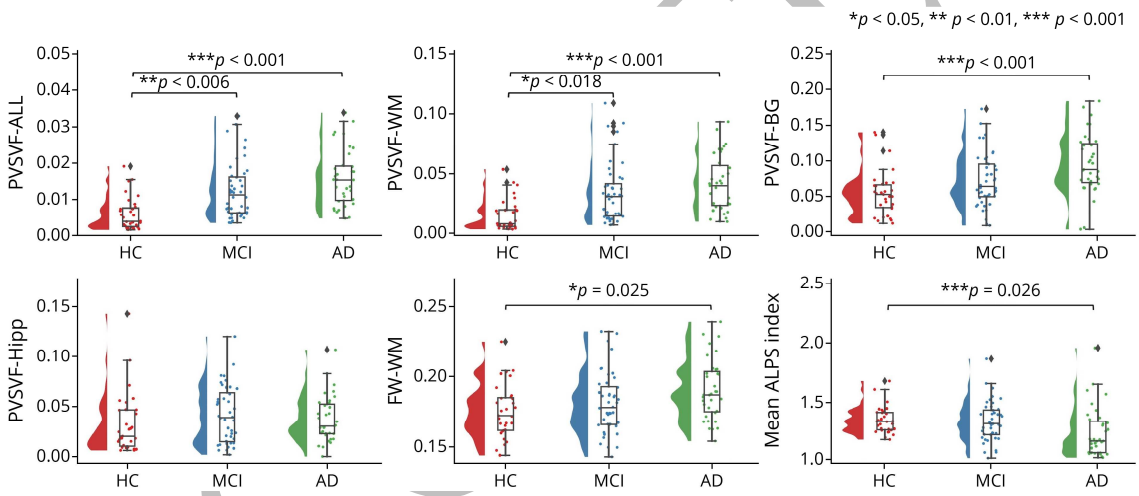

Figure 5. Correlation analyses. Relationships between variables that showed significant correlation in partial Spearman's rank correlation tests in the patients with MCI and Alzheimer's disease combined. Red lines depict linear regression with 95% confidence interval (shadow).

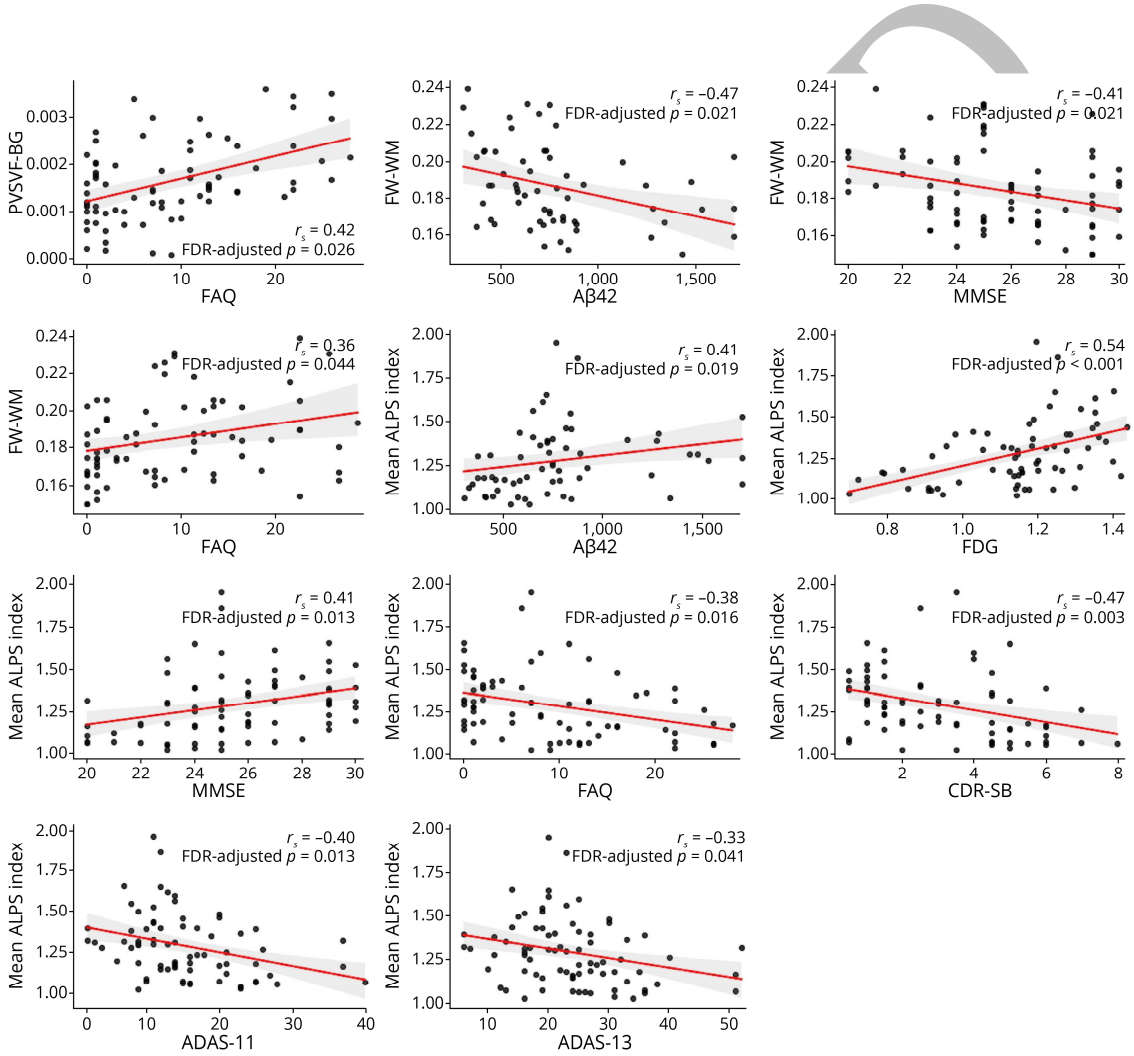

Neurology®

Association of MRI Indices of Glymphatic System With Amyloid Deposition and Cognition in Mild Cognitive Impairment and Alzheimer Disease

Koji Kamagata, Christina Andica, Kaito Takabayashi, et al.

Neurology published online September 19, 2022
DOI 10.1212/WNL.0000000000201300